Journal of Engineering and Technology for Industrial Applications

ITEGAM-JETIA

Manaus, v.10 n.49, p. 71-79. September/October., 2024.
DOI: https://doi.org/10.5935/jetia.v10i49.1221

ISSN ONLINE: 2447-0228

RESEARCH ARTICLE OPEN ACCESS

ADVANCED DUAL-LOOP CONTROL ARCHITECTURE FOR SUPERIOR PMSM PERFORMANCE UTILIZING FINITE-CONTROL-SET MODEL PREDICTIVE CONTROL AND EXPONENTIAL REACHING LAW SLIDING MODE CONTROL

Djaloul Karboua[1], Youcef Chouiha[2], Ben Ouadeh Douara [3], Ibrahim Farouk Bouguenna [4], Said Benkaihoul[5] and Belgacem Toual[6]

[1, 6] dept. Electrical Engineering–LASER Lab, Djelfa University Djelfa, Algeria.
[2,3,5] dept. Electrical Engineering–LAADI Lab, Djelfa University Djelfa, Algeria.
[4] Institute for Electrical Engineering University of Mascara Mascara, Algeria

[1] http://orcid.org/0000-0003-0155-9925, [2] http://orcid.org/0000-0001-9055-8953, [3] http://orcid.org/0000-0002-0548-5305,
[4] http://orcid.org/0000-0001-8631-8172, [5] http://orcid.org/0000-0002-8824-9761, [6] http://orcid.org/0000-0001-6900-9925,

Email: djaloul.karboua@univ-djelfa.dz , y.chouiha@univ-djelfa.dz , b.douara@univ-djelfa.dz , i.bouguenna@univ-mascara.dz , saidbenkaihoul@gmail.com , Toualb@gmail.com

ARTICLE INFO

Article History
Received: July 26th, 2024
Received: September 18th, 2024
Accepted: September 18th, 2024
Published: October 04th, 2024

Keywords:
PMSM,
Dual-Loop Control,
Robust technique,
ERL-SMC,
FCS-MPC.

ABSTRACT

This article contributes to the field by providing a comprehensive dual-loop control solution that addresses the limitations of individual control techniques and offers a robust and efficient framework for advanced PMSM control. In the current loop, FCS-MPC is employed to predict the future behavior of the motor currents and select the optimal control action from a finite set of possible inputs. This method ensures minimal current ripple, improved tran sient response, and efficient handling of the non-linearities and constraints inherent in PMSM operation. The predictive nature of FCS-MPC allows for real-time optimization, enhancing the overall efficiency of the current regulation. For the speed loop, the ERL-SMC is designed to provide robust control against parameter variations and external dis turbances. The exponential reaching law ensures a faster and smoother reaching phase, reducing chattering and improving the steady-state performance. By incorporating an ERL, the sliding mode controller can swiftly bring the system states to the sliding surface and maintain them, thus achieving high accuracy in speed tracking and robust performance under various operating conditions. The combination of FCS-MPC and ERL-SMC harnesses the predictive capabilities and op timization of the former with the robustness and disturbance rejection of the latter. This hybrid control strategy is evaluated through extensive simulations in MATLAB/Simulink. The simulation results demonstrate significant improvements in dynamic response, tracking accuracy, reduced overshoot, and enhanced disturbance rejection. Additionally, the proposed approach shows superior performance in handling sudden load changes and parameter uncertainties, confirming its po tential for high-performance PMSM drive applications.

I. INTRODUCTION

Permanent Magnet Synchronous Motors (PMSMs) have become a cornerstone in various industrial applications due to their high efficiency, power density, and excellent performance characteristics. These motors are particularly valued in applications demanding precise speed and position control, such as robotics, electric vehicles, and aerospace technologies. To fully exploit the advantages of PMSMs, vector control strategies are crucial for effective management of the current and speed loops [1-4].

FieldOriented Control (FOC) is one of the most widely used methods for controlling PMSMs. FOC decouples the torque

and flux components, allowing independent control of the motor's d-axis and q-axis currents. However, despite its popularity, FOC suffers from several limitations. The implementation of FOC requires precise tuning of PI controllers and accurate knowledge of motor parameters, making it complex and challenging in practical scenarios. Additionally, FOC is highly sensitive to parameter variations, which can degrade control accuracy and stability. The method also tends to have a slower dynamic response compared to more advanced control techniques. Another conventional method is Direct Torque Control (DTC), which directly controls the motor's torque and flux without the need for coordinate transformation. DTC offers faster dynamic response but comes with its own set of drawbacks. It often results in significant torque and flux ripple, leading to increased acoustic noise and mechanical stress. Furthermore, the nonconstant switching frequency in DTC complicates the design of power electronic converters, and like FOC, DTC's performance is sensitive to motor parameter variations [5-8]. Sliding Mode Control (SMC) is known for its robustness against parameter variations and external disturbances. Classical SMC ensures that the system states reach and remain on a predefined sliding surface. However, the main issue with classical SMC is chattering, which refers to high frequency oscillations caused by the discontinuous control action. Chattering can cause wear and tear in mechanical components and increase energy losses. Additionally, designing an effective sliding surface and reaching law in classical SMC requires careful tuning, which can be complex and application-specific [9-12]. Exponential Reaching Law-based Sliding Mode Control (ERL-SMC) addresses some of the shortcomings of classical SMC. By modifying the reaching law, ERL-SMC aims to reduce chattering and improve control performance. The exponential reaching law provides a continuous control action during the reaching phase, significantly reducing chattering. This approach also enhances robustness against disturbances and parameter variations and offers better steady-state accuracy and dynamic response compared to classical SMC. It also provides maintaining high-speed tracking accuracy and enhancing system stability under varying operating conditions [13], [14].

FiniteControl-Set Model Predictive Control (FCS-MPC) is a cutting-edge control strategy that has gained significant attention in recent years due to its ability to handle complex control problems with a high degree of precision. Unlike traditional control methods that rely on continuous control signals, FCS-MPC operates by predicting the future behavior of the system over a finite time horizon and selecting the optimal control action from a discrete set of possible inputs. This approach enables FCS-MPC to effectively manage non-linearities and system constraints, providing enhanced control performance. The predictive nature of FCS-MPC allows for the anticipation of future states, leading to improved transient responses and reduced steady-state errors. Furthermore, FCS-MPC's ability to minimize current ripple and optimize power efficiency makes it particularly suitable for applications in Permanent Magnet Synchronous Motor (PMSM) drives, where precision and efficiency are paramount. By continuously updating the control inputs based on real-time system feedback, FCS-MPC ensures that the control objectives are met with minimal deviation, thereby offering a robust and adaptive control solution for modern electrical drive systems [15-17]. To overcome the limitations of these conventional control methods, this paper proposes a dual-loop control strategy for PMSM drives. This strategy integrates FiniteControl-Set Model Predictive Control (FCS-MPC) for the current loop with Exponential Reaching Law-based Sliding Mode Control (ERL-SMC) for the speed loop. By combining FCS-MPC for the current loop and ERL-SMC for the speed loop, the proposed dualloop control strategy aims to harness the predictive capabilities and optimization of FCS-MPC with the robustness and disturbance rejection of ERL-SMC. This hybrid approach is validated through extensive simulations in MATLAB/Simulink, demonstrating significant improvements in dynamic response, tracking accuracy, and overall system robustness compared to conventional control method based on ERL-SMC. This study provides a comprehensive dual-loop control solution that addresses the limitations of individual control techniques and offers a robust and efficient framework for advanced PMSM control. The structure of this paper is organized as follows: Section 2 focuses on constructing a comprehensive model of the Permanent Magnet Synchronous Motor (PMSM) system. In Section 3, we detail the design of the Exponential Reaching Law Sliding Mode Controller (ERL-SMC) specifically for the PMSM speed loop, emphasizing its robustness and performance improvements. Section 4 is dedicated to the design of the Finite Control Set Model Predictive Control (FCS-MPC) for the PMSM current loop, highlighting its predictive capabilities and control accuracy. Following the control design sections, Section 5 presents the simulation setup and results, providing a thorough discussion on the effectiveness and efficiency of the proposed control strategies. Finally, Section 6 concludes the paper and summarizing the key findings.

II. CONSTRUCTING A MODEL OF THE PMSM SYSTEM

Before implementing any control strategy, it is imperative to transform the three-phase Permanent Magnet Synchronous Motor (PMSM) system into a two- phase representation using the Park transformation. The adoption of a d-q rotor reference frame significantly simplifies the derived equations, expediting the numerical calculations essential for computational simulations. This simplification not only accelerates the computational process but also ensures the constancy of resultant variables during steady-state operation, thereby facilitating subsequent computations and streamlining the design of the control system. Moreover, the d-q model within the rotor reference frame is widely recognized and favored in current literature due to its simplicity and applicability. Assumptions within this model include a cage-free rotor, sinusoidal back-EMF, negligible saturation, and minimal eddy current and hysteresis losses [18], [19]. Additionally, to utilize the nonlinear model effectively, the PMSM system is described by Equation 1, where the state variables comprise the stator speed, direct current, and quadrature current [20],[21].

$$\begin{cases} \dfrac{di_d}{dt} = \dfrac{1}{L_d}.\left(u_d - R_s.i_d + L_q.\omega_r.i_q\right) \\ \dfrac{di_q}{dt} = \dfrac{1}{L_q}\left(u_q - R_s.i_q - L_d.\omega_r.i_d - \omega_r.\Phi_f\right) \\ \dfrac{d\omega_r}{dt} = \dfrac{3.p^2}{2.J}\left(\Phi_f.i_q + \left(L_q - L_d\right)i_d i_q - \dfrac{\mathrm{F}}{J}.\omega_r - \dfrac{p}{J}.T_l\right) \\ \dfrac{d\theta_r}{dt} = \omega_r \end{cases} \quad (1)$$

i_d, i_q are d-q axis equivalent stator currents ; u_d, u_q are d-q axis equivalent stator voltages ; θ_r, ωr are rotor position and rotor speed ; p is number of pole pairs ; R_s is per phase stator resistance; L_d, L_q are d-q axis equivalent stator inductance ; T_e, T_l are electromagnetic and load torques ; J is moment of inertia of the rotor ; F is friction constant of the rotor and Φ_f is rotor magnetic flux linking the stator.

III. DESIGNING THE ERL-SMC FOR THE PMSM SPEED LOOP

Sliding mode control primarily aims to establish a switching surface that adheres to principles of existence, convergence, and stability. This involves adjusting the system's structure to guide the state trajectory towards this surface. Systems with adaptable structures undergo changes during operation. Sliding mode control typically operates in two modes: convergence towards the surface and subsequent sliding along it. Once the system reaches the switching surface, it follows a dynamic described by the sliding mode, asymptotically moving towards the equilibrium point within a finite time frame. The synthesis of sliding mode control methodically addresses performance and stability concerns. Implementation of this control entails three key steps: selecting the sliding surface, defining sliding conditions, and calculating the SMC law.the general formula for sliding surfaces is designed as follows [22-25]:

$$S(x,t) = \left(\frac{d}{dt} + \lambda\right)^{n-1} e(t) \tag{2}$$

Where λ is a positive number chosen by the designer (a parameter that fixes the dynamic of the error in sliding mode), n is system order, $S(x,t)$ is the sliding surface and $e(t)$ is tracking error. Once the sliding surface is established, the system trajectory is directed towards the origin, eventually reaching it asymptotically, as dictated by the sliding condition described in the following equation [26]:

$$\frac{1}{2}\frac{d}{dt}S^2 \leq \eta|S| \tag{3}$$

Where $\eta > 0$ Following the establishment of the sliding surface and adherence to the sliding condition, the control law is determined through a two-phase approach. Firstly, the sliding phase is enacted to ensure the system remains on the sliding surface, achieved by designing an equivalent term where $S(x,t) = 0$ and $\dot{S}(x,t) = 0$. Subsequently, the approach phase is initiated to meet the sliding condition, accomplished by formulating a switching law where $S(x,t) \neq 0$ and $S(x,t) = 0$. The specific design of the SMC control law unfolds as [27]:

$$u = u_{eq} + u_s \tag{4}$$

Using the exponential approach law, one can reduce the occurrence of rapid oscillations in the control signal while preserving the dynamic performance of the sliding mode arrival process through careful adjustment of parameters k_1 and k_2. However, if k_2 is set too high, it may result in undesirable chattering. To overcome this problem the ERL-SMC has been improved using the Pseudo-sliding mode based on continuous approximation [14],[28]. Similarly, within this context, the speed tracking error and the sliding surface can be expressed as follows:

$$\begin{cases} e_\omega = \omega_r^{ref} - \omega_r \\ S_\omega = \omega_r^{ref} - \omega_r \end{cases} \tag{5}$$

With reference to the sliding phase outlined earlier, the equivalent termtakes on the following expression:

$$i_{q-eq}^{ref} = \frac{2.J}{3.p^2.\Phi_f}.\left(\dot{\omega}_r^{ref} + \frac{F}{J}\omega_r + \frac{p}{J}.T_l\right) \tag{6}$$

Given the preceding approach phase, the switching term based on ERL-SMC and Pseudo-sliding mode is delineated as follows:

$$u_s = k_1.tgh(S_\omega) + k_2.S_\omega \tag{7}$$

Where S is sliding surface of SMC and k_1 , k_2, are the gains used to regulate the ERL based on Pseudo sliding mode controller. The control law for the PMSM's speed loop, based on the ERL-SMC, can be formulated using the equiv alent and switching terms as follows:

$$i_q^{ref} = i_{q-eq}^{ref} + i_{q-s}^{ref} \tag{8}$$

IV. DESIGNING OF THE FCS-MPC FOR THE PMSMCURRENT LOOP

Predictive control is a control strategy that relies on a dynamic mathematical model of the system to forecast future behavior. It optimizes control inputs over a specified time horizon by considering system dynamics, constraints, and desired objectives. The con troller updates its predictions and optimizations in real time, adapting to changes and disturbances to achieve optimal performance. This method is widely used in complex systems requiring precise and adaptive con trol, such as industrial processes, robotics, and energy systems. Key features of this type of controller include selecting the best actions by minimizing a cost function and using a system model to predict future variable behavior over a set time horizon. A summary of the Model Predictive Control (MPC) operating principle is illustrated in Figure 1. Using the system model and the available measurements up to time k, future state values are projected until a predetermined horizon at time k + N. By minimizing the cost function, the optimal sequence of actions is determined, and the first action in this sequence is implemented. This procedure is repeated at each sampling instant, incorporating the most recent data. The prediction model used is a discrete-time model, expressed in the following state space form [16-17].

$$\begin{cases} x(k+1) = A.x(k) + B.u(k) \\ y(k) = C.x(k) + D.u(k) \end{cases} \tag{9}$$

A cost function that reflects the desired system behavior must be defined. This function takes into account future states, control actions, and reference values.

$$J = f(x(k), u(k), \ldots\ldots, u(k+N)) \tag{10}$$

The objective of the MPC optimization problem is to minimize the cost function *J* over a specified time horizon *N*, while considering constraints and the system model. This process results in a series of *N* optimal control actions, but only the first action in the sequence is implemented by the controller. At each sampling instant, new measured data is used to resolve the optimization problem, generating a new set of optimal control actions each time. This approach is known as receding horizon control [17].

$$u(k) = [1\ 0\ \ldots 0]\ arg\ min_u J \tag{11}$$

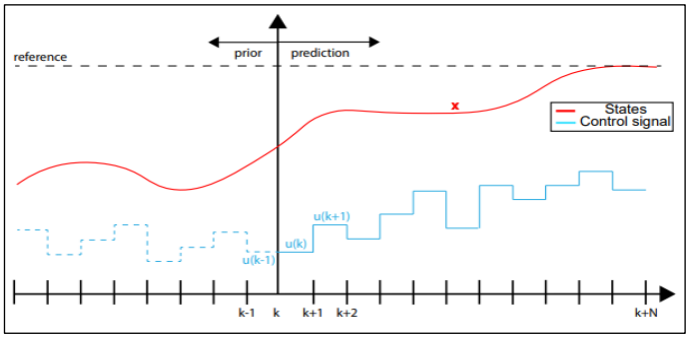

Figure 1: MPC principle of working.
Source: Authors, (2024).

In this paper, the PMSM is connected to a widely used three-phase source inverter, as shown in Figure 2. This inverter has eight distinct switching vectors, re sulting in eight voltage vectors, u_0 to u_7. There are two zero vectors and six nonzero vectors. The amplitudes of the active voltage vectors in the stationary reference frame $\alpha\beta$ are illustrated in Table 1 and Figure 1

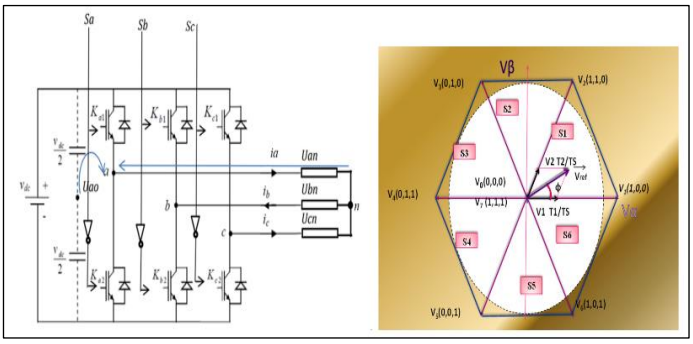

Figure 2: PMSM Feeding Structure with Two-Level Voltage Source Inverter and Voltage Vector Design.
Source: Authors, (2024).

To develop the Finite Control Set Model Predictive Control (FCS-MPC), a discrete-time model is required to predict the currents at a future sample period.

Table 1: Different switching modes and corresponding voltage vector of the voltage source converter.

Conducting Modes	**Switching States**			**Output Voltage**	
	Sa	*Sb*	*Sc*	*Uα*	*Uβ*
U_0	0	0	0	0	0
U_1	1	0	0	$\frac{2V_{dc}}{3}$	0
U_2	1	1	0	$\frac{V_{dc}}{3}$	$\frac{\sqrt{3}V_{dc}}{3}$
U_3	0	1	0	$-\frac{V_{dc}}{3}$	$\frac{\sqrt{3}V_{dc}}{3}$
U_4	0	1	1	$\frac{2V_{dc}}{3}$	0
U_5	0	0	1	$-\frac{V_{dc}}{3}$	$-\frac{\sqrt{3}V_{dc}}{3}$
U_6	1	0	1	$\frac{V_{dc}}{3}$	$-\frac{\sqrt{3}V_{dc}}{3}$
U_7	1	1	1	0	0

Source: Authors, (2024).

Therefore, the forward Euler method is applied to the continuous-time model (1) with a sampling time period T_s [in seconds]. For small $T_s \ll 1$, the following approximations hold: $x(k) = x(kTs) \approx x(t)$ and $\frac{d}{dt}x(t) \approx \frac{x(k+1)-x(k)}{Ts}$ for all $t \in [kTs, (k+1)Ts]$ and $k \in \mathbb{N} \cup \{0\}$. Consequently, the discrete-time representation of the PMSM in the rotating (d-q) reference frame can be expressed as follows [29] [30]:

$$\begin{cases} i_d(k+1) = \left(1 - \frac{R_s T_s}{L_d}\right) i_d(k) + T_s \omega_e(k) i_q(k) + \frac{T_s}{L_d} u_d(k) \\ i_q(k+1) = \left(1 - \frac{R_s T_s}{L_q}\right) i_q(k) - T_s \omega_e(k) i_d(k) + \frac{T_s}{L_q} u_q(k) - \frac{\psi_p T_s}{L_q} \omega_e(k) \end{cases} \quad (12)$$

The stator voltage udq of the PMSM can be represented as a function of the inverter's switching vector $S_{abc}[k] \in \{0,1\}^3$. Here's the revised version of the equation [16]:

$$v_{dq}(k) = T_p(\theta_e)^{-1} . T_C . \frac{1}{3} v_{dc}[k] . v_{abc} \quad (13)$$

With;

$$\begin{cases} T_p(\theta_e)^{-1} = T_{dq0 \to \alpha\beta 0} \\ T_C = T_{\alpha\beta 0 \to abc} \\ v_{abc} = \begin{bmatrix} 2 & -1 & -1 \\ -1 & 2 & -1 \\ -1 & -1 & 2 \end{bmatrix} . S_{abc}[k] \end{cases} \quad (14)$$

Where $T_{dq0 \to \alpha\beta 0}$ and $T_{\alpha\beta 0 \to abc}$ represent the inverse Park and Clarke transformations, respectively. v_{dc} denotes the DC-bus voltage (in V), and v_{abc} indicates the stator voltage in the abc frame (in V). θ_e represents the electrical rotor position of the PMSM, given by the integral of Ω with respect to time. The discrete-time predictive model anticipates the behavior of seven vectors as outlined in equation 12. Subsequently, throughout the sampling period, these seven predicted vectors are evaluated to identify the states that minimize the cost function and result in the lowest absolute error between the reference and predictive currents $(i_d[k+1], i_q[k+1])$ [31]. The formulation of the cost function is defined as follows:

$$g = \left|i_d{}^*[k+1] - i_d[k+1]_{u_{0,\dots 7}}\right| + \left|i_q{}^*[k+1] - i_q[k+1]_{u_{0,\dots 7}}\right| + \begin{cases} 0 \ if \ \sqrt{i_d[k+1]^2 + i_q[k+1]^2} \le i_{max} \\ \infty \ if \ \sqrt{i_d[k+1]^2 + i_q[k+1]^2} > i_{max} \end{cases} \quad (15)$$

The first segment indicates the reduction in reactive power, the second segment pertains to tracking the torque-producing current, and the final segment deals with the maximum permissible stator current of the PMSM. The maximum allowable current for the direct and quadrature axes, represented as i_{max}, applies to both the d and q axes. The future reference currents $i_d^*[k+1]$ and $i_q^*[k+1]$ are predicted using Lagrange extrapolation based on previous sampling points [k], [k1], and [k2], as noted in [16]. The reduction in reactive power is covered in the initial segment, the tracking of the torque-producing current is addressed in the second segment, and the final segment outlines the maximum permissible

stator current of the PMSM. The maximum current for the quadrature axis (q) and the direct axis (d) is indicated by i_{max}. The future reference currents $i_d^*[k+1]$ and $i_q^*[k+1]$ are estimated using Lagrange extrapolation based on prior sampling points [k], [k1], and [k2], as detailed in [16].

$$i_{dq}{}^*[k+1] = 3i_{dq}{}^*[k] - 3i_{dq}{}^*[k-1] + i_{dq}{}^*[k-2] \quad (16)$$

V. SIMULATION, RESULTS AND DISCUSSION

To demonstrate the effectiveness of the dual-loop control studied in this paper for the PMSM, a simulation model was built in Matlab/Simulink, as shown in Figure 3 for the ERLSMC with FCS-MPC. These controls are applied to the speed and current loops of the PMSM. To validate the dual-loop control, various scenarios are presented to prove its effectiveness. The selection of design parameters was based on a thorough analysis of PMSM performance using several criteria: stability, performance characteristics, robustness, cost function, and energy minimization. The PMSM parameters used in this work are listed in Table 2.

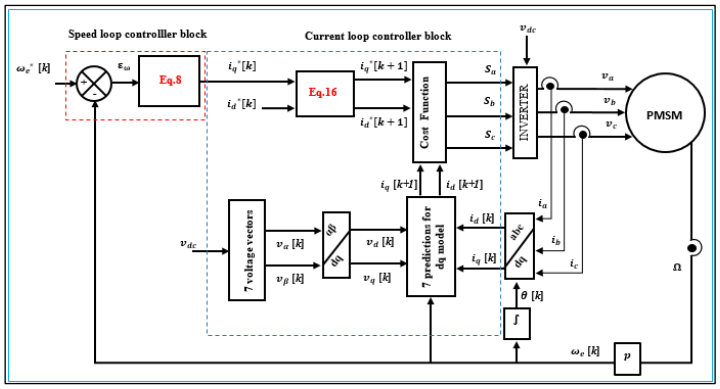

Figure 3: Scheme of PMSM controller based on a novel dual-loop control design.
Source: Authors, (2024).

Table 2: Parameters of the PMSM drive.

PMSM's parameters		
R_s=0.6 Ω	L_d =1.4 10^{-3} H	L_q=2.8 × 10^{-3} H
F =1.4 × 10^{-3} $M.m.s^{-1}$	Φ_f =12× 10^{-2} Wb	J =1.1 × 10^{-3} $kg.m2$
v_{dc} = 100V		p=4

Source: Authors, (2024).

In the first scenario, the PMSM operates in a stable state with the speed stabilized at a medium level (600 rpm) and a load torque of 5 N·m applied. This scenario showcases the performance of speed, torque, and the direct and quadratic currents. Additionally, a comparison is made between the classical PMSM drive design based on the ERL-SMC and the novel PMSM drive design based on the dual-loop control. As shown in Figure 4, the speed performance indicates that the novel design based on the dualloop control outperforms the classical design based on the ERLSMC in terms of rise time (Tr) and steady-state error (SSE). The rise time for the novel design is approximately 6 ms, whereas the classical design has a rise time of approximately 12 ms. The steady-state error for the novel design is around 0.006%, compared to 0.05% for the classical design. Moreover, the novel design is stabilized with minimal chattering, while the classical design suffers from significant chattering. Specifically, the chattering for the novel design is between +0.055 and -0.035, while for the classical design, it is between +0.15 and -0.85.

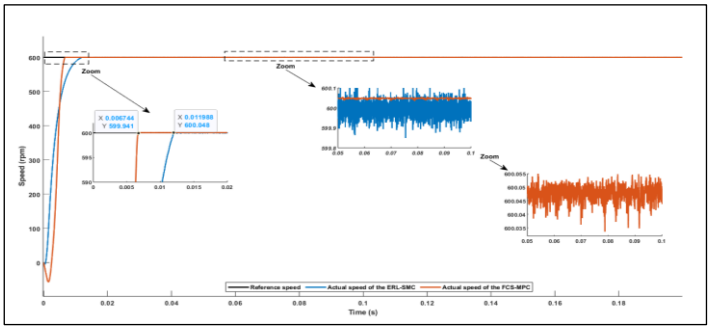

Figure 4: PMSM speed performance under the first scenario.
Source: Authors, (2024).

Regarding the electromagnetic torque performance illustrated in Figure 5, the novel design significantly minimizes torque ripple compared to the traditional ERL-SMC design, which experiences substantial torque ripple. The torque ripple in the novel FCSMPC design ranges between +0.15 and -0.15, while the ERLSMC design exhibits a torque ripple range between +0.55 and - 0.5. Moreover, Figure 6 highlights the superior performance of the novel design in terms of direct and quadratic current control. The tolerance band for the direct current in the novel control design is notably narrower than that of the ERL-SMC. Specifically, the tolerance band for the direct current in the novel control design is between +0.15 and -0.15, whereas for the ERL-SMC, it is between +0.5 and -0.5. These estimates are similarly applicable to the quadratic current.

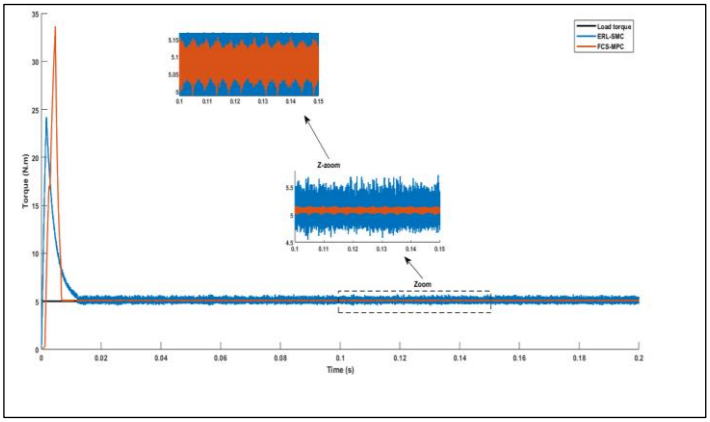

Figure 5: PMSM electromagnetic torque performance under the first scenario.
Source: Authors, (2024).

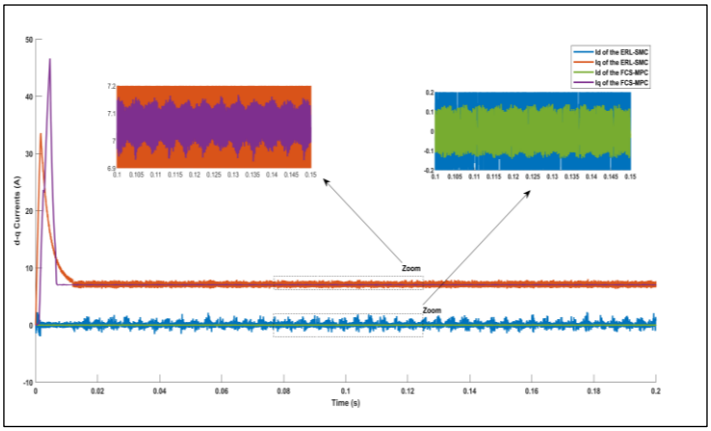

Figure 6: PMSM d-q currents performance under the first scenario.
Source: Authors, (2024).

The second scenario is presented to demonstrate the robustness of the novel control design under external disturbances. Various load torque values (1 N.m, 2 N.m, 5 N.m, and 3 N.m) were applied at different time instances, as shown in Figure 8. Under these conditions, the novel control design exhibits superior speed performance compared to the classical ERA-SMC design. Although the rise time remains consistent with the first scenario for both controls, overshoots and undershoots occur during changes in load torque. The overshoot/undershoot rate in the novel control design is limited to 0.6%, which is significantly lower than that of the classical control design, as illustrated in Figure 7. Regarding electromagnetic torque performance, depicted in Figure 8, the novel control design outperforms the classical control design with substantially lower steady-state error and reduced chattering. Additionally, Figure 9 shows that the novel control design maintains excellent performance in terms of direct and quadratic currents. This results in high-quality electrical power, reduced noise, lower losses, and improved stability under external disturbances.

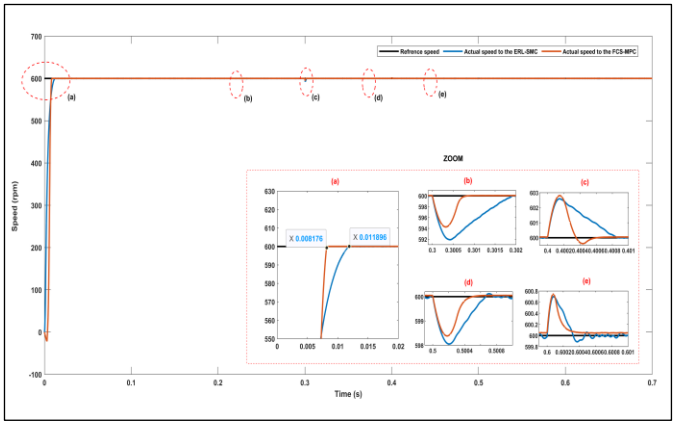

Figure 7: PMSM speed performance under the second scenario.
Source: Authors, (2024).

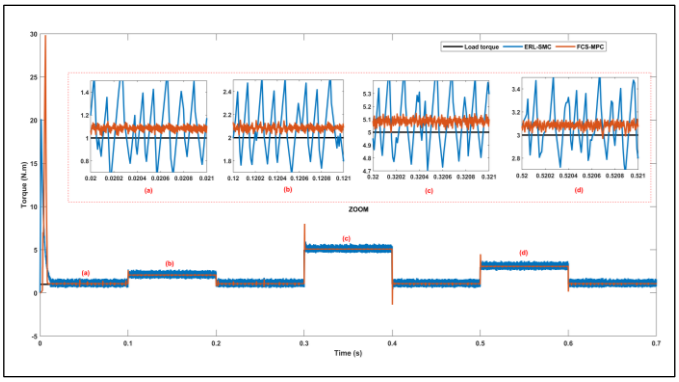

Figure 8: PMSM electromagnetic torque performance under the second scenario.
Source: Authors, (2024).

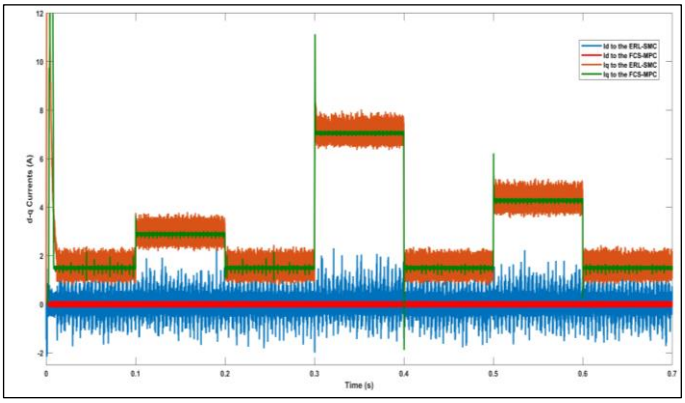

Figure 9: PMSM d-q currents performance under the second scenario.
Source: Authors, (2024).

The three-phase current performance is significantly enhanced with the novel control design, which effectively minimizes current oscillations and maintains stability within a consistent tolerance band during load torque variations, as demonstrated in Figure 10. In contrast, the classical control design exhibits inferior performance for the three-phase current, characterized by a wider tolerance band and reduced stability during load torque changes. Detailed information regarding the current performance of both control designs is provided in Figures 10 and 11. This senario examines the robustness of the novel control design under parameter uncertainties.

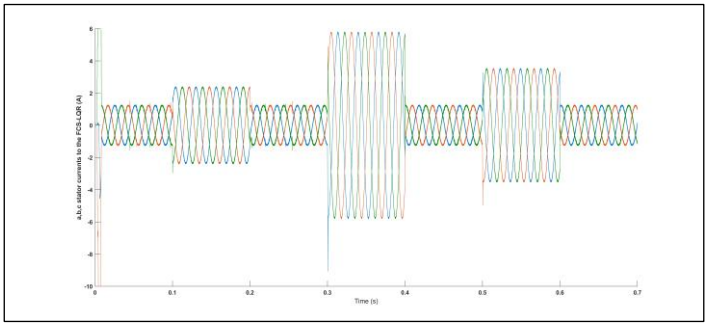

Figure 10: PMSM a,b,c currents performance based on the novel control design under the second scenario.
Source: Authors, (2024).

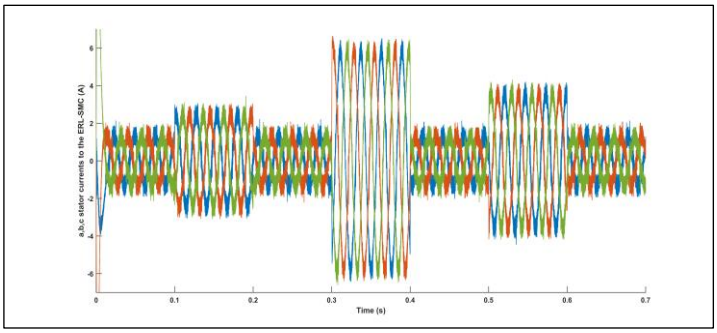

Figure 11: PMSM a,b,c currents performance based on the classical control design under the second scenario.
Source: Authors, (2024).

The variations in PMSM parameters, including resistance, direct and quadratic inductances, and inertia, were studied at increasing rates. Figure 12 illustrates this scenario, showing changes at 0%, 50%, 100%, 150%, and 200% with a medium speed of 600 rpm. Additionally, the novel control performs well in terms

of the uncertainty rate (UR) for the change in rise time across the different percentages of PMSM parameter changes, with the UR estimated at 0.004096 seconds. Furthermore, the novel control design exhibits a very small steady-state error. The steady-state error percentage between the reference speed and the 200% uncertainty level is estimated at 0.025%, between the reference speed and the 0% uncertainty level at 0.008%, and between the 0% and 200% uncertainty levels at 0.01.

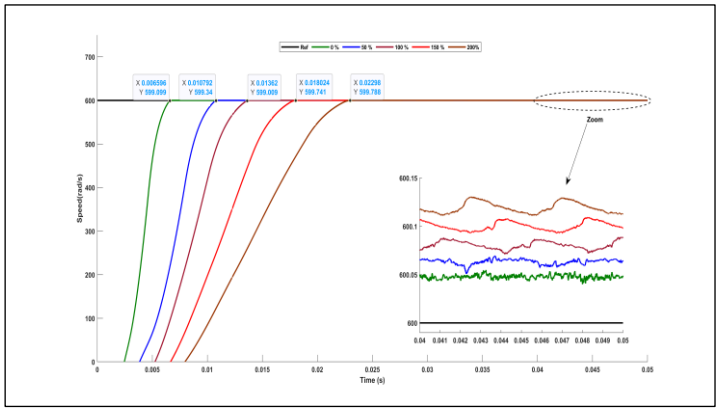

Figure 12: PMSM speed performance under the uncertainties scenario.
Source: Authors, (2024).

The final scenario tests the speed performance of the PMSM using the novel control design at high speed levels. This novel control design is compared to the classical ERL-SMC-based control design. This scenario is particularly challenging because the PMSM operates across vastly different speed ranges, with each range representing a distinct operational state and large changes in rotational speed between states. Under this scenario, the durability of the studied controls is evaluated. Figure 13 illustrates the high performance of the PMSM, where the speed varies between low (50 rpm), medium (375 rpm), and high (1000 rpm). This analysis explores the performance characteristics and phenomena that might impede the PMSM's performance, as well as the control design's flexibility in adapting to changes in speed levels from one state to another.

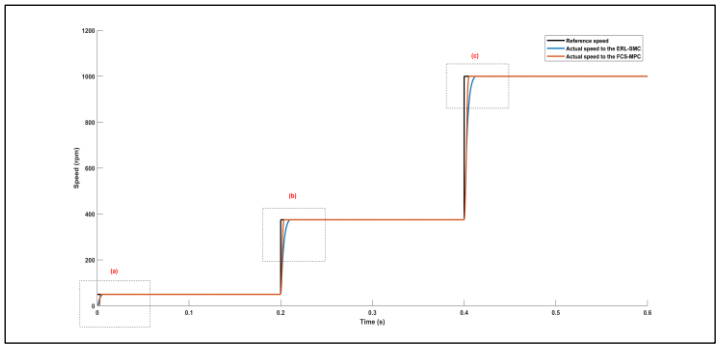

Figure 13: PMSM speed performance under the speed levels changes.
Source: Authors, (2024).

To determine which technique performs better, we will analyze each speed level individually. Figure 14 focuses on region (a) from Figure 13, showcasing the speed performance of the PMSM at a low speed of 50 rpm, with a comparative study of the mentioned techniques. According to Figure 14 and Table 3, the novel control design outperforms the classical ERL-SMCbased control design in terms of performance characteristics and durability. The novel control design achieves the smallest steadystate error, estimated at 0.02%, as well as the littest rise time, estimated at 3.2ms

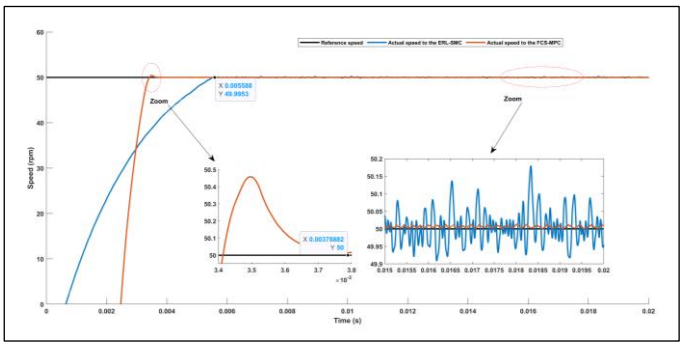

Figure 14: PMSM speed performance under the low speed level.
Source: Authors, (2024).

The second level involves transitioning to medium speed and evaluating the PMSM speed as it moves from slow to medium operation. Figure 15 and Table 3 focus on region (b) from Figure 13, highlighting the PMSM's performance at a medium speed of 375 rpm. At this level, the novel control design excels in speed performance characteristics compared to the classical control design. The rise time during application is estimated at 3.5 ms, the steady-state error is 0.007%, and stability is optimal with the novel control design. These results indicate that the novel control design is highly suitable for medium speed, particularly when transitioning from low to medium speed.

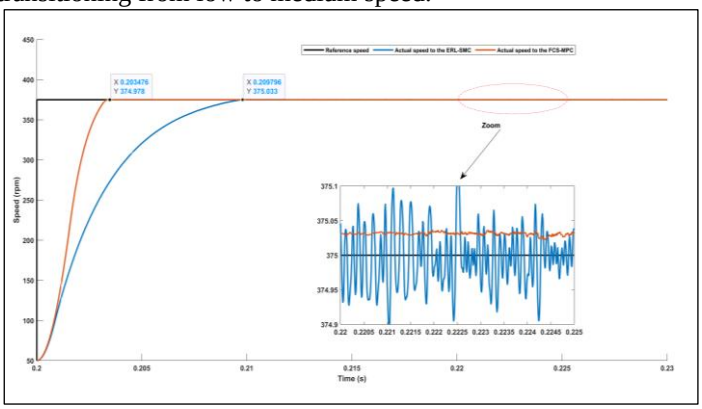

Figure 15: PMSM speed performance under the medium speed level.
Source: Authors, (2024).

Figure 16 and Table 3 highlight region (c) from Figure 13, illustrating the transition to the third level, representing the highest performance speed of 1000 rpm. Despite this abrupt change from medium to high speed, the novel control design demonstrates superior durability and performance characteristics for the PMSM compared to the classical ERL-SMC control design. A detailed analysis of performance characteristics, based on Figures 13, 14, 15, 16, and Table 3, reveals that the average rise time for the novel control design is estimated at 4 ms, while the classical control design is 9.2 ms. The average uncertainties in speed performance are estimated at 0.8 ms for the novel control design and 3.3 ms for the classical control design. Thus, the novel control design outperforms the classical control design in most speed performance characteristics.

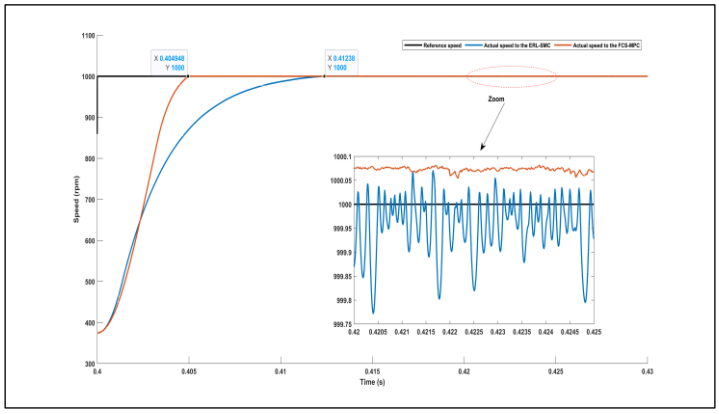

Figure 16: PMSM speed performance under the high speed level.
Source: Authors, (2024).

Table 3: Performance characteristics comparison under variation of speed levels between the novel control design (ncd)and the classical control design based on (CCD) ERL-SMC.

Performance Characteristics	NCD	CCD
Rise Time (ms)		
Low speed	3.789	5.588
Medium speed	3.5	9.8
High speed	4.9	12.2
Steady-state error (%)		
Low speed	0.04	0.4
Medium speed	0.01	0.03
High speed	0.008	0.02
Performance Stability	Medium stable	Little stability

Source: Authors, (2024).

VI. CONCLUSIONS

This paper presents a novel dual-loop control strategy for enhancing PMSM performance, utilizing Finite Control Set Model Predictive Control (FCS-MPC) for the current loop and Exponential Reaching Law Sliding Mode Control (ERL-SMC) for the speed loop. The innovative control design has demonstrated superior performance under various conditions, including uncertainties, disturbances, and changes in speed levels.The FCSMPC method effectively predicts future motor current behavior and selects optimal control actions, resulting in minimal current ripple, improved transient response, and efficient handling of the non-linearities and constraints inherent in PMSM operation. Concurrently, the ERL-SMC provides robust control against parameter variations and external disturbances, ensuring accurate speed tracking and reduced chattering. Extensive simulations in MATLAB/Simulink confirm that the novel dual-loop control design significantly outperforms the classical ERL-SMC-based control design. It exhibits excellent characteristics in terms of dynamic response, tracking accuracy, reduced overshoot, and enhanced disturbance rejection. The novel control approach also shows exceptional capability in managing sudden load changes and parameter uncertainties, further validating its potential for high-performance PMSM drive applications. Overall, this study contributes a robust and efficient dual-loop control framework that leverages the strengths of both FCS-MPC and ERL-SMC, offering a substantial improvement over traditional control methods and advancing the field of PMSM control systems.

VII. AUTHOR'S CONTRIBUTION

Conceptualization: Djaloul Karboua, Youcef Chouiha, Ben ouadeh Douara, Ibrahim Farouk Bouguenna, Said Benkaihoul and Belgacem Toual
Methodology: Djaloul Karboua, Youcef Chouiha, Ben ouadeh Douara, Ibrahim Farouk Bouguenna, Said Benkaihoul and Belgacem Toual
Investigation:
Discussion of results: Djaloul Karboua, Youcef Chouiha, Ben ouadeh Douara, Ibrahim Farouk Bouguenna, Said Benkaihoul and Belgacem Toual
Writing – Original Draft: Djaloul Karboua, Youcef Chouiha, Ben ouadeh Douara, Ibrahim Farouk Bouguenna, Said Benkaihoul and Belgacem Toual
Writing – Review and Editing: Djaloul Karboua, Youcef Chouiha, Ben ouadeh Douara, Ibrahim Farouk Bouguenna, Said Benkaihoul and Belgacem Toual
Resources: Djaloul Karboua, Youcef Chouiha, Ben ouadeh Douara, Ibrahim Farouk Bouguenna, Said Benkaihoul and Belgacem Toual
Supervision: Djaloul Karboua, Youcef Chouiha, Ben ouadeh Douara, Ibrahim Farouk Bouguenna, Said Benkaihoul and Belgacem Toual
Approval of the final text: Djaloul Karboua, Youcef Chouiha, Ben ouadeh Douara, Ibrahim Farouk Bouguenna, Said Benkaihoul and Belgacem Toual

VIII. REFERENCES

[1] D. Fu, X. Zhao, and H. Yuan, "High-precision motion control method for permanent magnet linear synchronous motor", IEICE Electronics Express, vol. 18, no. 9, pp. 20210097–20210097, 2021. https://doi.org/10.1587/elex.18.20210097

[2] B. K. Bose, "Power electronics and motion control-technology sta tus and recent trends", IEEE Transactions on Industry Applications, vol. 29, no. 5, pp. 902–909, 1993. https://doi.org/10.1109/28.245713

[3] Y. Pan, X. Liu, Y. Zhu, B. Liu, and Z. Li, "Feedforward decoupling control of interior permanent magnet synchronous motor with genetic algorithm parameter identification", Progress In Electro magnetics Research M, vol. 102, pp. 117–126, 2021. https://doi.org/10.2528/PIERM21032903

[4] W. Li, "Application of pmsm control in electric vehicle", Internal Combustion Engine & Parts, vol. 298, no. 22, pp. 51–52, 2019.

[5] J.-W. Jung, V. Q. Leu, T. D. Do, E.-K. Kim, and H. H. Choi, "Adap tive pid speed control design for permanent magnet synchronous motor drives", IEEE Transactions on Power Electronics, vol. 30, no. 2, pp. 900–908, 2014. https://doi.org/10.1109/TPEL.2014.2311462

[6] J. Hu, J. Zou, F. Xu, Y. Li, and Y. Fu, "An improved pmsm rotor position sensor based on linear hall sensors", IEEE Transactions on Magnetics, vol. 48, no. 11, pp. 3591–3594, 2012. https://doi.org/10.1109/TMAG.2012.2202279

[7] W. Liu, S. Chen, and H. Huang, "Adaptive nonsingular fast terminal sliding mode control for permanent magnet synchronous motor based on disturbance observer", IEEE Access, vol. 7, pp. 153791 153798, 2019. https://doi.org/10.1109/ACCESS.2019.2948945

[8] X. Zhang, L. Sun, K. Zhao, and L. Sun, "Nonlinear speed control for pmsm system using sliding-mode control and disturbance compensation techniques", IEEE transactions on power electronics, vol. 28, no. 3, pp. 1358–1365, 2012. https://doi.org/10.1109/TPEL.2012.2206610

[9] K. Mei and S. Ding, "Second-order sliding mode controller design subject to an upper-triangular structure", IEEE Transactions on Systems, Man, and Cybernetics: Systems, vol. 51, no. 1, pp. 497 507, 2018. https://doi.org/10.1109/TSMC.2018.2875267

[10] Y. Shtessel, M. Taleb, and F. Plestan, "A novel adaptive-gain su pertwisting sliding mode controller: Methodology and application", Automatica, vol. 48, no. 5, pp. 759–769, 2012. https://doi.org/10.1016/j.automatica.2012.02.024

[11] Z. Zhou, B. Zhang, and D. Mao, "Robust sliding mode control of pmsm based on rapid nonlinear tracking differentiator and disturbance observer", Sensors, vol. 18, no. 4, p. 1031, 2018. https://doi.org/10.3390/s18041031

[12] C. Xie, J. Wu, Z. Guo, Y. Wang, and J. Liu, "Sensorless control of vehicle-mounted pmsm based on improved sliding mode observer", in Journal of Physics: Conference Series, vol. 2030, no. 1. IOP Publishing, 2021, p. 012004. https://doi.org/10.1088/1742-6596/2030/1/012004

[13] D. Karboua, B. Toual, A. Kouzou, B. O. Douara, T. Mebkhouta, and A. N. Bendenidina, "High-order supper-twisting based terminal sliding mode control applied on three phases permanent syn chronous machine", Periodica Polytechnica Electrical Engineering and Computer Science, vol. 67, no. 1, pp. 40–50, 2023. https://doi.org/10.3311/PPee.21026

[14] D. Karboua, B. Toual, B. O. Douara, T. Mebkhouta, M. L. Benaissa, and Y. Chouiha, "Expansion switching law based sliding mode applied on a three-phase permanent magnet synchronous machine", in 2022 2nd International Conference on Advanced Electrical Engineering (ICAEE). IEEE, 2022, pp. 1–6. https://doi.org/10.1109/ICAEE53772.2022.9961993

[15] I. F. Bouguenna, A. Tahour, R. Kennel, and M. Abdelrahem, "Multiple-vector model predictive control with fuzzy logic for pmsm electric drive systems", Energies, vol. 14, no. 6, p. 1727, 2021. https://doi.org/10.3390/en14061727

[16] J. Rodriguez and P. Cortes, "Predictive control of power converters and electrical drives", John Wiley & Sons, 2012. https://doi.org/10.1002/9781119941446

[17] J. A. Andersson, J. Gillis, G. Horn, J. B. Rawlings, and M. Diehl, "Casadi: a software framework for nonlinear optimization and op timal control", Mathematical Programming Computation, vol. 11, pp. 1–36, 2019. https://doi.org/10.1007/s12532-018-0139-4

[18] P. Pillay and R. Krishnan, "Modeling of permanent magnet motor drives," IEEE Transactions on industrial electronics", vol. 35, no. 4, pp. 537–541, 1988. https://doi.org/10.1109/41.9176

[19] T. P. Kumar and P. Samyuktha, "Vector control drive of permanent magnet synchronous motor using resolver sensor", International Journal of Computer Science Engineering (IJCSE), vol. 2, no. 04, 2013.

[20] M. Nicola, C.-I. Nicola, and D. Selis, teanu, "Improvement of pmsm sensorless control based on synergetic and sliding mode controllers using a reinforcement learning deep deterministic policy gradient agent", Energies, vol. 15, no. 6, p. 2208, 2022. https://doi.org/10.3390/en15062208

[21] R. Abdessemed, "Modélisation et simulation des machines électriques: électrotechnique", Ellipses, 2011.

[22] W. Perruquetti and J. P. Barbot, "Sliding mode control in engineer ing", Marcel Dekker New York, 2002, vol. 11. https://doi.org/10.1201/9780203910856

[23] W. Gao, Y. Wang, and A. Homaifa, "Discrete-time variable struc ture control systems," IEEE transactions on Industrial Electronics, vol. 42, no. 2, pp. 117–122, 1995. https://doi.org/10.1109/41.370376

[24] D. Karboua, T. Belgacem, Z. H. Khan, C. Labiod, and I. K. Ibraheem, "Toward an optimal twisting-sliding mode control of a three-phase pmsm for electric vehicles", Advances in Mechanical Engineering, vol. 15, no. 9, p. 16878132231198664, 2023. https://doi.org/10.1177/16878132231198664

[25] J. Guldner and V. Utkin, "The chattering problem in sliding mode systems", in Proc. 14th Int. Symp. of Mathematical Theory of Networks and Systems (MTNS), 2000.

[26] J.-J. E. Slotine, W. Li et al., "Applied nonlinear control", Prentice hall Englewood Cliffs, NJ, 1991, vol. 199, no. 1.

[27] K. Djaloul, T. Belgacem, I. Atif, C. Youcef, M. Toufik, and D. B. Ouadeh, "High order sliding mode control based on a new terminal strategy applied on the speed permanent magnet synchronous ma chine", in 2023 XIX International Scientific Technical Conference Alternating Current Electric Drives (ACED). IEEE, 2023, pp. 1–6. https://doi.org/10.1109/ACED57798.2023.10143468

[28] Y.-G. Huangfu, "Research of nonlinear system high order sliding mode control and its applications for pmsm", Ph.D. dissertation, Northwestern Polytechnical University (Chine), 2010.

[29] X. Gao, M. Abdelrahem, C. M. Hackl, Z. Zhang, and R. Kennel, "Direct predictive speed control with a sliding manifold term for pmsm drives", IEEE Journal of Emerging and Selected Topics in Power Electronics, vol. 8, no. 2, pp. 1258–1267, 2019. https://doi.org/10.1109/JESTPE.2019.2923285

[30] M. Abdelrahem, C. Hackl, R. Kennel, and J. Rodriguez, "Sen sorless predictive speed control of permanent-magnet synchronous generators in wind turbine applications", in PCIM Europe 2019; International Exhibition and Conference for Power Electronics, Intelligent Motion, Renewable Energy and Energy Management. VDE, 2019, pp. 1–8.

[31] Y. Zhang, D. Xu, J. Liu, S. Gao, and W. Xu, "Performance improvement of model-predictive current control of permanent magnet synchronous motor drives", IEEE Transactions on Industry Applications, vol. 53, no. 4, pp. 3683–3695, 2017. https://doi.org/10.1109/TIA.2017.2690998